IEEE Access
Multidisciplinary | Rapid Review | Open Access Journal

Received October 24, 2018, accepted November 22, 2018, date of publication November 27, 2018,
date of current version December 27, 2018.

Digital Object Identifier 10.1109/ACCESS.2018.2883494

Broadband Circularly Polarized Filtering Antennas

YAZHOU DONG[1,2,3], STEVEN GAO[3], (Senior Member, IEEE), QI LUO[3], (Member, IEEE), LEHU WEN[3], CHUN-XU MAO[4], SHI-WEI DONG[2], (Senior Member, IEEE), XIAOJUN LI[2], GAO WEI[1], GEYI WEN[5], (Member, IEEE), YOULING GENG[6], AND ZHIQUN CHENG[6]

[1]School of Electronics and Information, Northwestern Polytechnical University, Xi'an 710129, China
[2]National Key Laboratory of Science and Technology on Space Microwave, China Academy of Space Technology (Xi'an), Xi'an 710100, China
[3]School of Engineering and Digital Arts, University of Kent, Canterbury CT2 7NZ, U.K.
[4]School of Electrical Engineering and Computer Science, The Pennsylvania State University, PA 16801, USA
[5]Nanjing University of Information Science and Technology, Nanjing 210044, China
[6]College of Electronics and Information, Hangzhou Dianzi University, Hangzhou 310018, China

Corresponding author: Steven Gao (s.gao@kent.ac.uk)

This work was supported in part by the EPSRC under Grant EP/P015840/1 and Grant EP/N032497/1, in part by the National Natural Science Foundation of China under Grant 61801374 and Grant 51777168, in part by the National Key Laboratory of Science and Technology on Space Microwave under Grant 6142411020302, and in part by the Scholarship of the China Scholarship Council under Grant 201704980035.

ABSTRACT This paper consists of two parts. The first part presents a review of the recent development in broadband circularly polarized filtering antennas. The second part presents a novel design of broadband integrated filtering antenna based on eighth-mode SIW (EMSIW) resonators for rectenna applications. This work has three main novel contributions. First, by adjusting the external quality factors and coupling coefficients of the resonators in this filtering antenna, optimum input impedance with a complex value can be realized within the filtering antenna. Thus there is no need for an external impedance matching network, which is usually required between the antenna and the rectifying circuits; Second, compared with traditional microstrip resonators, high-Q EMSIW cavities are used to increase antenna gain; third, the coupling gap between the EMSIW resonators also acts as the feeding structure of the radiator. So the feeding structures are all on the middle layer. The ground plane on the back side is a complete structure without any defects. This novel structure design improves front-to-back ratio to enhance the antenna receiving efficiency. To validate this method, two C-band circularly polarized integrated filtering antennas with an input impedance of 50 Ω and complex impedance are designed, simulated, and fabricated. The measured results show that the operating frequency bandwidth of the proposed antennas is more than 14.5% at C-band with the gain above 8 dBi. The 3-dB axial ratio bandwidth is larger than 8.5% and the front-to-back ratio is higher than 18 dB. Moreover, the proposed antenna with complex impedance is conjugate matched with the input impedance of a specific rectifying circuit at 5.8 GHz and harmonics suppression at the second-harmonic frequency is achieved.

INDEX TERMS Broadband antenna, circularly polarized antenna, impedance match, filtering antenna, rectenna.

I. INTRODUCTION

The development of modern wireless systems demands radio frequency (RF) front-ends and antennas with compact sizes, light weight, low cost and multiple functions. In traditional designs, passive components such as filters, power dividers and antennas are designed separately and then cascaded. This approach leads to some problems including bulky volumes, heavy weight, complicated structures and high insertion loss between the components. In recent years, filtering antenna has become a hot topic of research due to its potential of overcoming these problems [1]–[6]. In the filtering antenna, the antenna becomes one element of the filtering circuit which usually consists of many resonant units. Thus the filtering antenna requires the antenna and the filtering circuits be designed, simulated and optimized simultaneously. Compared with traditional antennas, the integrated filtering

antenna does not require a separate impedance matching network between the antenna and the filtering circuits. In addition, it has many advantages such as a compact size, low loss, the enhancement of antenna bandwidth, high frequency selectivity, wideband harmonic suppression, improved out-of-band rejection and reduced interferences.

Although much work has been done in filtering antenna/array research, most of the reported filtering antennas are linearly polarized (LP). One important application is to use the filtering antenna techniques to design circularly polarization antennas/arrays. Circularly polarized (CP) antennas do not require strict alignment between transmitting and receiving antennas. CP antennas can also combat the multipath fading and are immune to the 'Faraday rotation' effect due to the ionosphere. Because of the above features, circularly polarized antennas are very popular for various wireless systems such as satellite communication systems, global navigation satellite systems, and wireless power transmission systems [7]. The key challenges for circularly polarized filtering antenna design are to realize broad axial ratio (AR) bandwidth and high radiation efficiency. Meanwhile, it is also very important to investigate how to apply the circularly polarized filtering antenna in satellite/radar and microwave power transmission applications.

This paper focuses on the research of the broadband circularly polarized filtering antennas. The state-of-the-art broadband circularly polarized filtering antennas are briefly reviewed in Section II. Then, a novel design of broadband filtering antenna based on eighth-mode SIW (EMSIW) resonators for rectenna application is presented in Section III. To reduce the insertion loss and radiation loss of the traditional microstrip resonators, high-Q EMSIW cavities are used in the feeding system of the antenna. To conjugate match the rectifying circuit, the external quality factors and coupling coefficients of the resonators can be adjusted to realize complex impedance matching. In addition, the novel topology improves the front-to-back ratio to enhance the antenna efficiency. Section IV concludes this paper.

II. REVIEW OF BROADBAND CIRCULARLY POLARIZED FILTERING ANTENNAS

Most of the reported filtering antenna researches concerns LP antennas, and there is only a few works on CP filtering antennas in the literature [8]–[13]. Circularly polarized filtering antenna design involves more complicated parameter optimization and it is more challenging to realize broadband CP filtering antenna. In this section, several state-of-the-art circularly polarized filtering antennas including dielectric resonator antennas (DRA), monopole antennas and microstrip antennas, are reviewed.

A. WIDEBAND CP FILTERING DRAS

The dielectric resonator antenna is regarded as one of the ideal candidates for modern wireless systems because of its advantages such as low loss, a small size, and a wide bandwidth [14], [15]. Circularly polarized filtering DRAs with wideband operation have been investigated in recent years.

A wideband circularly polarized DRA with bandpass filtering and wide harmonic suppression was proposed in [8]. The configuration and photograph are shown in Fig. 1. A wideband filtering quadrature coupler based on a snowflake shaped patch was implemented to feed a hollow DRA. This structure could realize circular polarization and filtering function simultaneously. This antenna operated at 1.8 GHz and exhibited a wide bandwidth of 27.8% (AR $\leq$ 3 dB, RL ≤ -12.4 dB) with an average gain of 6 dBic. A rejection of over 19 dB was achieved in the suppression band up to the third harmonic. Another circularly polarized filtering DRA for X-band applications was presented in [9]. A rectangular ring slot was etched into the ground plane of the dielectric laminate to generate circular polarization. An additional semi-elliptical shaped filter was used to improve the selectivity. The antenna operated from 7.9 to 8.4 GHz with the gain around 5.3 dBic and 3 dB AR bandwidth of 3.68%.

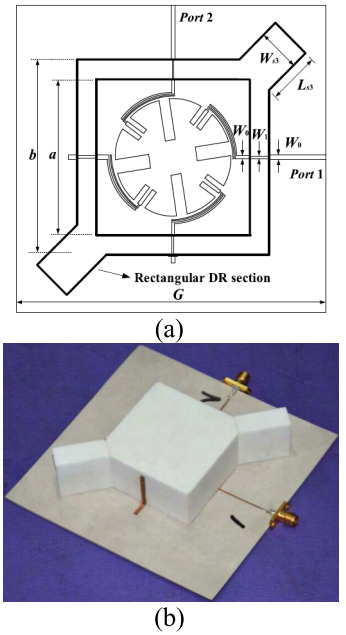

(a)

(b)

FIGURE 1. Configuration and photograph of the wideband CP filtering DRA reported in [8]: (a) the structure of quadrature coupler; (b) photograph.

B. CP FILTERING MONOPOLE ANTENNAS

Monopole antennas have the merits of compact sizes and omnidirectional radiations, which are important for the applications where omnidirectional radiation is required. Several LP filtering antennas based on monopole antennas had been well investigated in [16]–[18]. However, to the authors' best knowledge, there is only one design reported which realized the circular polarization. A circularly polarized monopole antenna with filtering function was proposed in [10] and shown in Fig. 2. A miniaturized coupled filter based on bent-loop resonators was integrated to realize filtering function,

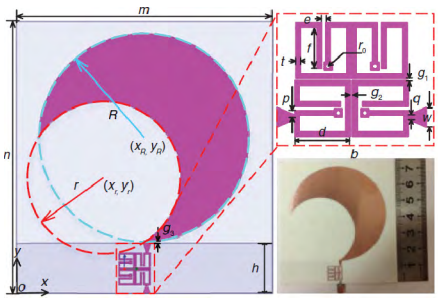

FIGURE 2. Configuration and photograph of the broadband CP filtering monopole antenna presented in [10].

while the falcate-shaped patch was adopted to obtain the circular polarization. This antenna exhibited good frequency selective performances, return loss and gains.

C. BROADBAND CP FILTERING MICROSTRIP ANTENNAS

Microstrip antennas have many advantages such as low profiles, lightweight and low cost. It is one of the most widely used antenna types. Therefore, the circularly polarized filtering microstrip antennas have been investigated extensively [11]–[13], [19], [20]. In this section, some latest typical examples are discussed.

A compact circularly polarized co-designed filtering antenna was reported in [11]. As shown in Fig. 3, this antenna was based on a patch radiator integrated with a bandpass filter. The filter was composed of coupled stripline open-loop resonators. The patch served as the radiator and the last stage resonator of the filter. The circular polarization was obtained by using dual feeds with 90 degrees phase delay. The filtering circuit with impedance matching functionality

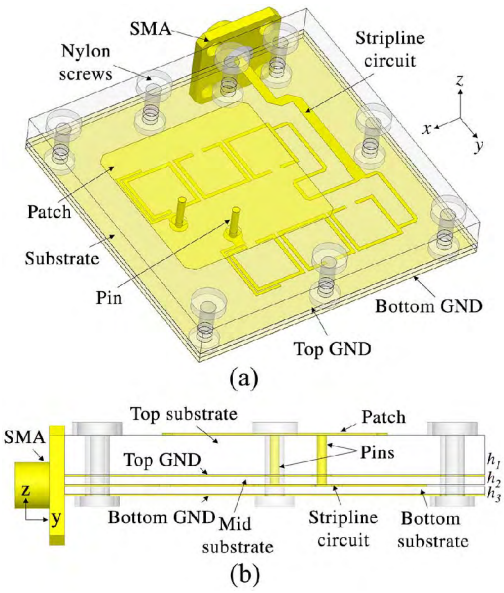

FIGURE 3. Structure of the broadband CP filtering microstrip antenna reported in [11]: (a) 3D view, (b) Side view.

improved both the impedance and axial ratio bandwidths. The return loss of the designed filtering antenna was below −13.5 dB over a bandwidth from 3.77 to 4.26 GHz (12.2%), with the axial ratio less than 3 dB and the gain higher than 5.2 dBic. However, this antenna had three substrate layers. Thus its structure is relatively complicated.

In [12], a dual-band CP microstrip array antenna with the shared aperture was developed for C-/X-band satellite communications. Fig. 4 shows the structure of the subarray. The antenna element was based on a novel technique of achieving CP using a single-feed dual-coupling structure. The circular patch was fed by a 50 Ω microstrip line via two U-shaped slots etched in the ground plane. At the end of the microstrip feed, a hairpin resonator was attached and coupled with the two U-slots. The antenna array shows a wide impedance bandwidth of 21% and 21.2% at C-band and X-band, respectively. The 3-dB AR bandwidths in C-band and X-band are 13.2% and 12.8%. However, due to the hairpin resonator placed on the back and two resonant U-slots in the ground plane, the front-to-back ratio is only −12dB.

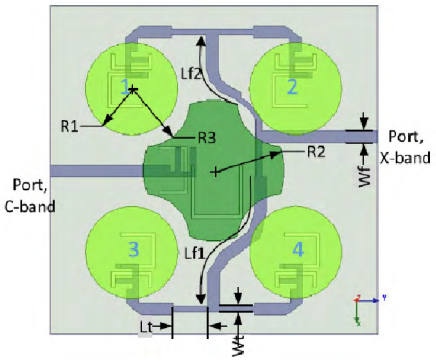

FIGURE 4. Configuration of the C/X-band CP filtering microstrip antenna subarray reported in [12].

Compared with the low-Q planar resonators, the integration of the high-Q resonators with antennas are more attractive in filtering antenna design, for their merits of lower insertion losses and better frequency selectivity. By integrating CP patch antenna with SIW cavity filters, a circularly polarized patch antenna with enhanced impedance and AR bandwidth was implemented in [13]. As shown in Fig. 5, a third-order SIW cavity based Chebyshev filter was embedded in the antenna to enhance the out-of-band rejection and bandwidths. By sequentially rotating the antenna elements, a 2 × 2 array was formed and an impedance-AR bandwidth of 8.3% was achieved.

III. CASE STUDY: BROADBAND CP FILTERING ANTENNA FOR RECTENNA APPLICATION

Wireless power transfer (WPT) overcomes the disadvantages of the traditional power supply using wired systems, and provide a more flexible power supply for various applications [21]–[24]. Microwave power transmission (MPT), as one of the key technologies in WPT, has demonstrated

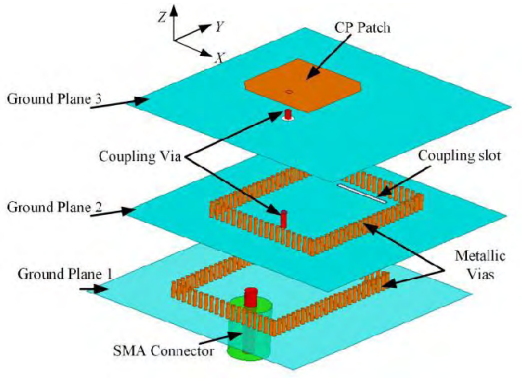

FIGURE 5. Exploded view of the broadband CP filtering microstrip antenna reported in [13].

the potential for power transmission over a long distance in many publications. In MPT system, rectenna array plays an important role in receiving and rectifying microwave energy. The design of the rectenna is essential for ensuring the overall efficiency of the MPT. A rectenna is usually composed of a receiving antenna unit and a rectifying circuit. Besides, a low-pass filter is always required between the receiving antenna and the rectifying circuit for suppressing harmonic re-radiation generated by diode nonlinearity [25]–[27].

To improve the integration of the rectenna, the receiving antenna with harmonic inhibition suppression can eliminate the use of low-pass filter in the rectifying circuit. A circularly polarized patch antenna with defect ground structure (DGS) under the microstrip feedline was proposed in [28] to avoid the harmonics. The double dumbbell-shaped DGS structure can suppress the harmonics. The reflection coefficient of this antenna is −30 dB at 5.8 GHz and −3 dB at the second harmonic 11.6 GHz. However, the bandwidth of this antenna is only 60MHz, and an extra impedance match network is needed. Another circularly polarized rectenna with harmonic suppression for WPT was presented in [29]. The substrate integrated waveguide structure was used to enhance the gain, and suppress surface wave. A shunt open stub was loaded on the feeding microstrip line to suppress harmonic. The gain is about 6.9 dBi and the bandwidth is about 100 MHz (5.75–5.85 GHz). An extra shorted single branch was then adopted to match the rectifying circuit.

Conventional rectenna designs usually suffer from the loss of filter, impedance matching network, and limited bandwidth. The concept of the integrated filtering antenna can be applied to rectenna design. As a case of study, a novel broadband CP filtering antenna based on EMSIW resonators is developed for rectenna application.

A. CONFIGURATION

Fig. 6 shows the structure of the proposed broadband circularly polarized filtering antenna. The antenna consists of two substrates of Rogers 4003 ($\varepsilon_r = 3.55$, $\tan\delta = 0.009$) with the thickness of 0.813 mm. The distance between the two substrates is $h = 2$mm. Viewing from the top, the radiator is a squared patch with two truncated corners for generating the circular polarization, as shown in Fig. 6 (b). Around the patch, four parasitic strips are introduced to improve the AR bandwidth.

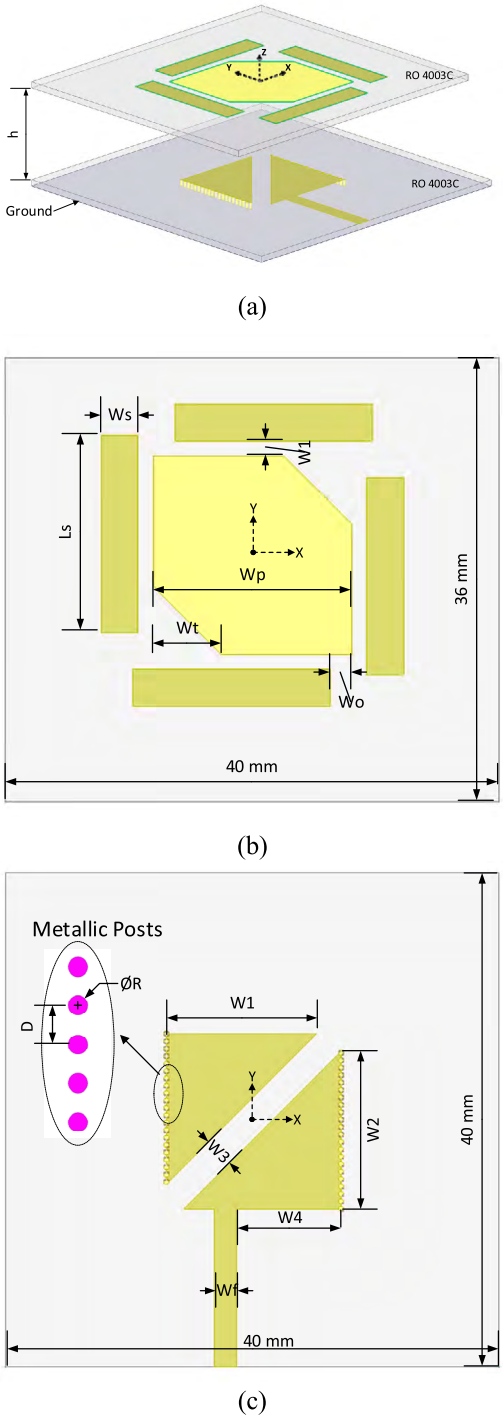

FIGURE 6. The configuration of the proposed CP filtering antenna: (a) exploded 3D view; (b) top view; (c) details of the feeding 1/8 SIW resonators.

The substrate integrated waveguide (SIW) technique has facilitated the design of cavity resonators with advantages

of high-Q, low loss, lightweight, easy fabrication and integration with planar circuits. However, the applications of SIW resonators are rarely in low-frequency bands due to their relatively large sizes. To overcome this problem, half-mode SIW (HMSIW), quarter-mode SIW (QMSIW), or even eighth-mode SIW (EMSIW) cavities have been proposed to reduce the size of the circuit [30]. The electric field distributions in the square SIW cavity, QMSIW cavity, EMSIW cavity resonating at the dominant mode TE101 and two coupled EMSIW resonators in the proposed antenna are displayed in Fig. 7, respectively. The resonant frequencies of the EMSIW resonators can be determined by [30]:

$$f_{TE101}^{EMSIW} = \frac{c}{2\pi\sqrt{\mu_r\varepsilon_r}}\sqrt{(\frac{\pi}{a_{eff}^{EMSIW}})^2+(\frac{\pi}{a_{eff}^{EMSIW}})^2} = \frac{c}{\sqrt{2\mu_r\varepsilon_r}a_{eff}^{EMSIW}} \quad (1)$$

$$a_{eff}^{EMSIW} = a_{eff}^{SIW} + \Delta w^{EMSIW} \quad (2)$$

where μ_r and ε_r are the relative permeability and relative permittivity of the resonator substrate, c is the speed of light and a_{eff}^{SIW} is the equivalent width of the original square SIW resonator. $\Delta w^{\mathbf{EMSIW}}$ are additional widths for EMSIW structures [31].

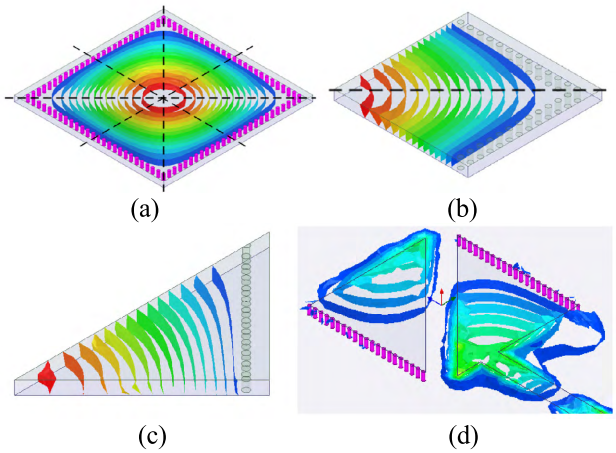

FIGURE 7. Field distributions in the (a) square SIW cavity, (b) QMSIW cavity, (c) EMSIW cavity resonating at the dominant mode TE101 and (d) two coupled EMSIW resonators.

In this antenna design, two EMSIW resonators are adopted in the feeding circuit as shown in Fig. 6 (c). The resonators are formed by connecting the triangle patches on the top layer and the ground plane on the bottom layer using closely spaced metallic vias. The diameter of the via is 0.3 to 0.4 mm, while the distance between the centers of vias is 0.6 to 0.8 mm, which is much smaller than the wavelength at the operating frequency (about 0.015 λ_0 @ 5.8 GHz) to prevent energy leaking from the sidewalls.

B. OPERATION PRINCIPLE

To illustrate the operation principle, a coupled-resonator topology of the broadband circularly polarized filtering antenna is shown in Fig. 8. The circles represent resonators and the solid lines represent the coupling between them. The EMSIW resonators are coupled through a gap with a width of W_3. The radiator on the top substrate is fed by the gap along the diagonal of the patch. The coupling can be adjusted by tuning the width of the gap. The EMSIW resonators are coupled and tuned with the patch to generate multiple resonant modes. As a result, the impedance bandwidth can be improved. The different resonant characteristics of these two types of resonators provide additional benefit of distinct harmonic frequencies [5]. This feature can be used to suppress the harmonics.

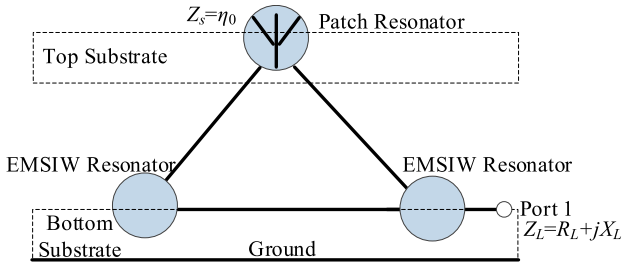

FIGURE 8. The topology of the proposed filtering antenna.

Four sequentially rotated rectangular strips are placed around the corner-truncated square patch to broaden the AR bandwidth [32]. The size of each parasitic strip is $L_s \times W_s$. The width of the gap between strips and patch sides is W_d and the distance from the patch corner to strip corner is W_o.

Since the input impedance of the rectifying diode is always complex, complex impedance matching should be achieved in the antenna design to eliminate the impedance match network with rectifying circuits. The simulation schematic of one rectifying circuit in ADS is shown in Fig. 9. The chosen rectifying diode is MA4E1317 manufactured by MACOM. The input impedance of the rectifying circuit is $73.5+j106.3\ \Omega$. The input impedance of the filtering antenna should be conjugated matched with it to achieve maximum power transfer. Based on the equivalent circuit model synthesis method of microwave filter, a complex impedance matching can be realized by adjusting the external quality factors and coupling coefficients of the filtering antenna.

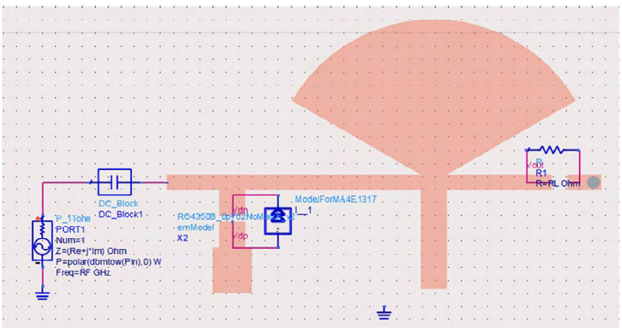

FIGURE 9. Simulation schematic of one rectifying circuit in ADS.

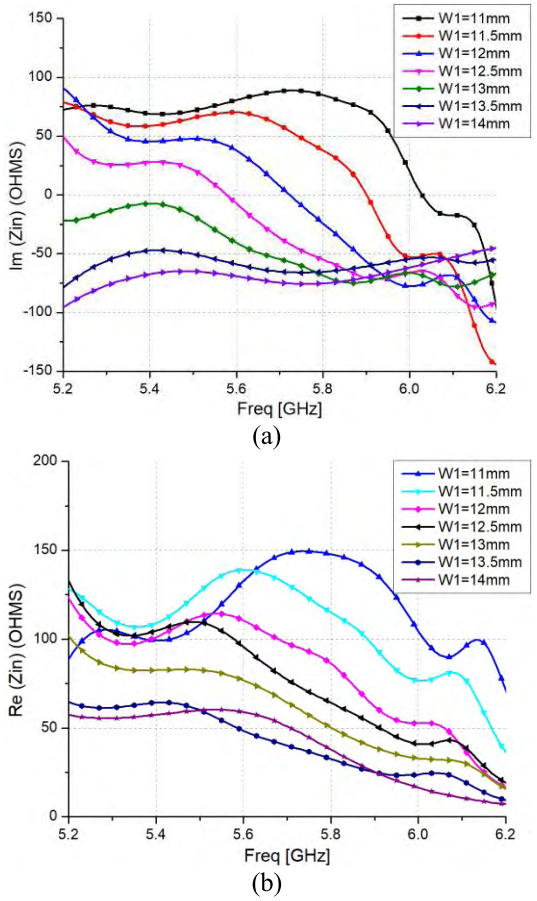

FIGURE 10. Variation of the input impedance of the antenna with different *W1*: (a) Imaginary part; (b) Real part.

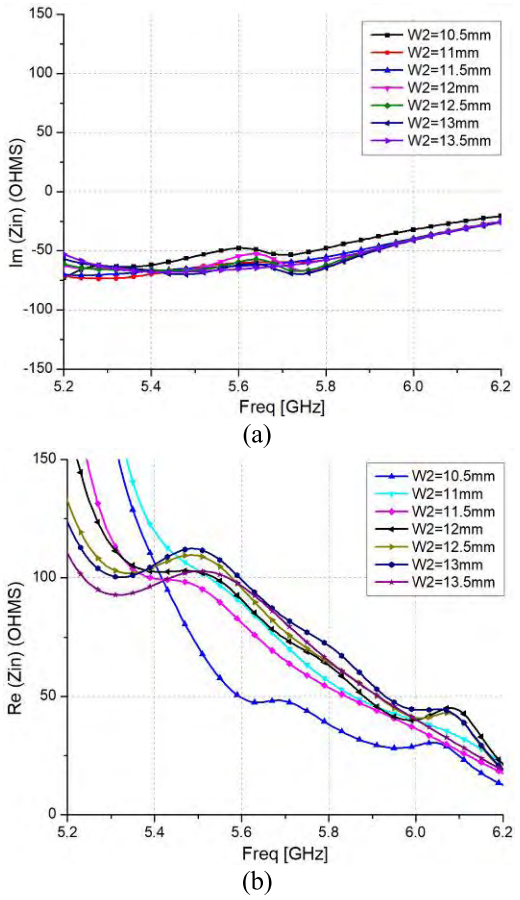

FIGURE 11. Variation of the input impedance of the antenna with different *W2*: (a) Imaginary part; (b) Real part.

Fig. 10 shows the simulated input impedance of the filtering antenna with different EMSIW cavity size as related to *W1*. As can be seen, both the imaginary part and real part of the input impedance vary with different *W1*. The real part of the input impedance can be tuned relatively independently with the parameters of *W2*, *W3*, *W4* and *Wp*. As shown in Fig. 11, the real part of the input impedance varies with different *W2*, while the imaginary part keeps relatively stable. The complex impedance of rectifying circuit that we used in the simulation of filtering antenna is a typical value. In addition, the input impedance of the filtering antenna can be easily tuned in our design method. Therefore, our antenna design can be easily adapted to the optimization of the rectifier circuit.

It should be noted that the coupling gap between the EMSIW resonators also acts as the feeding structure of the radiator. So the feeding structures are all on the middle layer. The ground plane on the backside is a complete structure without any defects. This novel structure design improves front-to-back ratio to enhance the antenna receiving efficiency.

Since the proposed design is based on stacked geometry, the parametric study of parameter *h* is also performed. The results can be seen in Fig. 12. The performance of the filtering antenna would be well while *h* is within the range

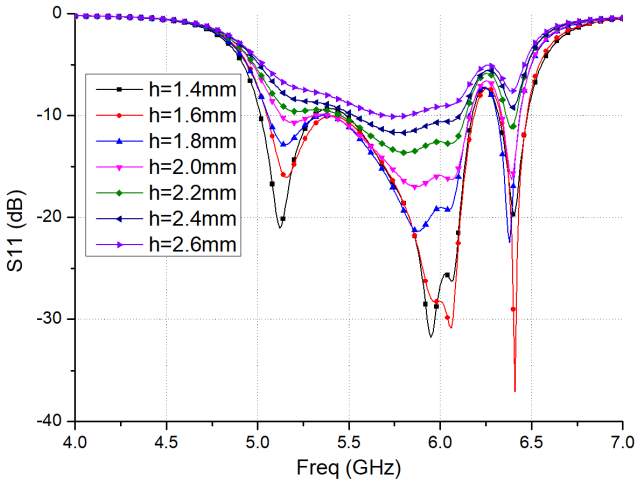

FIGURE 12. The results of parametric studies of parameter *h*.

of 1.4 to 2.4 mm. This requirement can be easily satisfied in PCB process.

The designs and optimizations of this type of filtering antennas with input impedance of 50 Ω and 73.5 – *j* 106.3 Ω are performed by using Ansoft HFSS and the optimized design parameters are shown in Table 1.

TABLE 1. Optimized Design Parameters (Units: mm).

Design Parameters	Matching for 50 Ω	Matching for 73.5 – j 106.3 Ω
h	2	2
W_p	17.5	16.1
W_t	4	5.5
L_s	16.5	16
W_s	4	3
W_d	2.5	1.2
W_o	3.3	1.8
$W1$	16.9	12.2
$W2$	10	12.7
$W3$	1.3	2.4
$W4$	2.4	8.5
Wf	1.82	1.82

C. VALIDATION AND RESULTS

To validate the design concept, two prototypes of the proposed antenna with input impedance of 50 Ω and 73.5 – j 106.3 Ω, denoted as Antenna 1 and Antenna 2 respectively, are fabricated and characterized. Fig. 13 shows the photos of the fabricated prototypes.

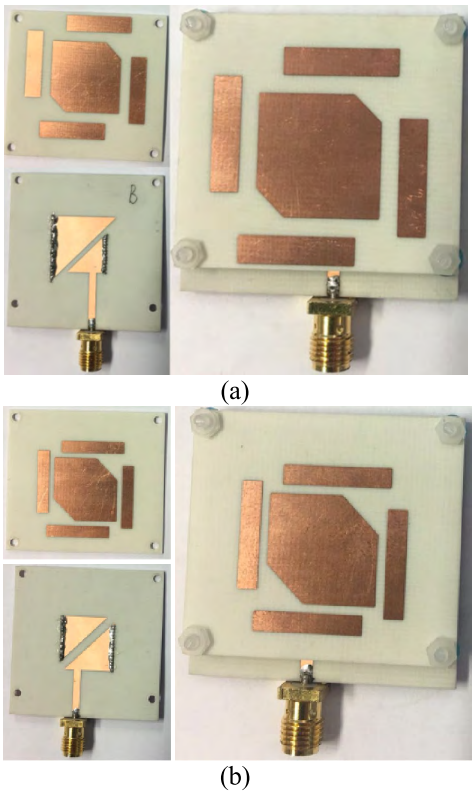

FIGURE 13. Photographs of the proposed antennas: (a) Antenna 1 with input impedance of 50 Ω; (b) Antenna 2 with input impedance of 73.5 – j 106.3 Ω.

The measured and simulated results of Antenna 1 with 50 Ω input impedance are shown in Fig. 14. The measured results agree well with the simulations except for some frequency shifts on a reflection zero point at high-frequency band. This is caused by the manufacture inaccuracy of the vias in EMSIW resonators. In the initial design, the diameter of the via R is 0.3 mm, and the distance between the centers of vias D is 0.6 mm. Due to the manufacturing process limitations in our workshop, the actual R is about 0.4 mm, and the actual D is about 0.8 mm. The simulated results in Fig. 14 illustrate this issue. A broadband impedance match from 5.15 to 6.20 GHz (fractional bandwidth ≈ 18.5%) is achieved. The filtering performance is very well except for a small glitch about −3 dB around 3.2 GHz. The value of $|S_{11}|$ is about −0.85 dB at the 2nd harmonic frequency band, which approximately ranges from 11 to 12 GHz.

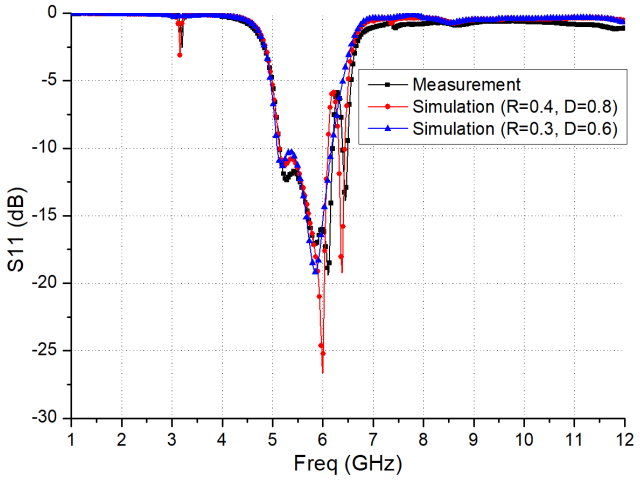

FIGURE 14. Measured and simulated S11 of Antenna 1.

The radiation patterns of the proposed antenna are measured in an anechoic chamber. The measured AR is below 3 dB from 5.5 to 6 GHz, as shown in Fig. 15. From Fig. 16, it can be seen that the antenna has a flat LHCP gain response of around 8.5 dBic from 5.5 to 6GHz. The gains are noticeably reduced by more than 18 dB from 11 to 12 GHz, exhibiting a good performance of 2nd harmonic suppression. Fig. 17 shows the simulated and measured radiation patterns of Antenna 1 in both the XOZ plane ($\phi = 0°$) and YOZ plane ($\phi = 90°$) at 5.5, 5.8, and 6 GHz, respectively. The antenna

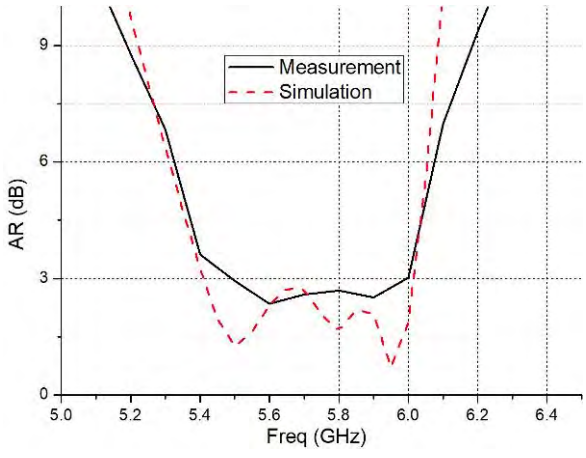

FIGURE 15. Measured and simulated AR of Antenna 1.

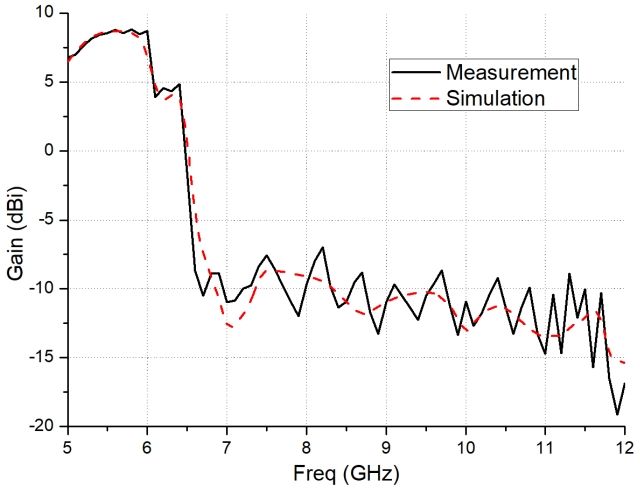

FIGURE 16. Measured and simulated gains of Antenna 1.

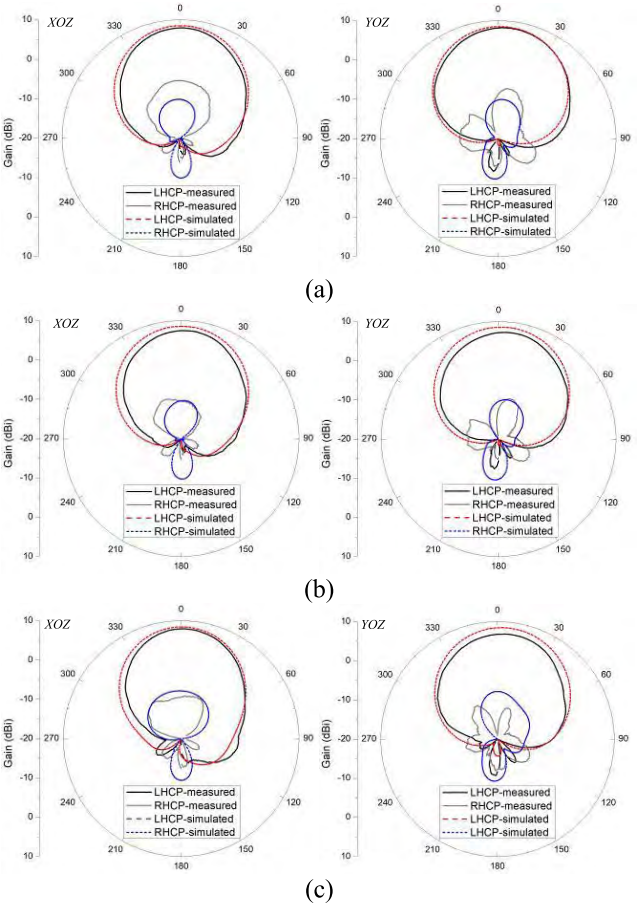

FIGURE 17. Radiation patterns of Antenna 1 in both the XOZ plane and YOZ plane: (a) 5.5 GHz; (b) 5.8 GHz; (c) 6 GHz.

has the consistent radiation patterns within the operating band. The measured cross-polarization discrimination (XPD) is over 16 dB in the broadside direction, and the measured front-to-back ratio is higher than 18 dB.

The simulated and measured results of Antenna 2 for complex input impedance are shown in Fig. 18 to 23.

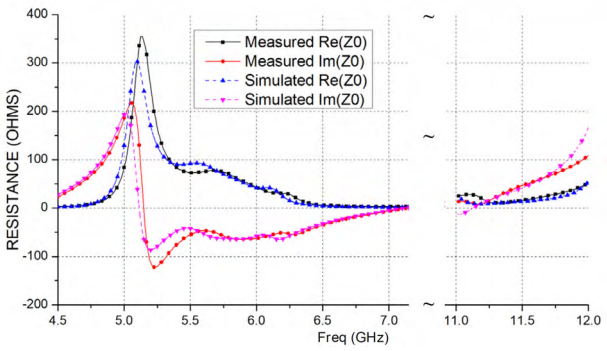

FIGURE 18. Measured and simulated input impedance of Antenna 2.

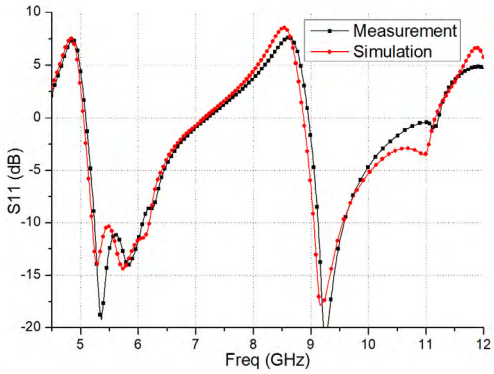

FIGURE 19. The re-calculated S11 of Antenna 2.

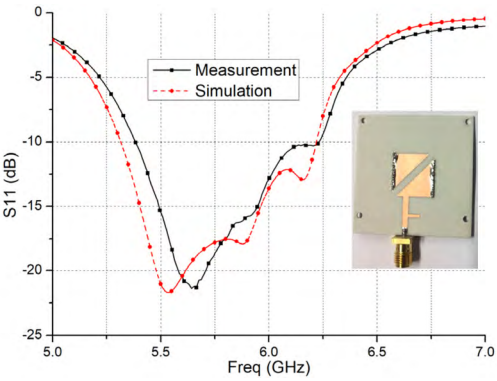

FIGURE 20. The open-shunt stub for anechoic chamber test system matching and its effect to S11.

Fig. 18 shows the measured and simulated input impedances of the Antenna 2, and the corresponding values of $|S_{11}|$ are also re-calculated based on system impedance $Z_0 = 73.5 - j\,106.3\ \Omega$ and is shown in Fig. 19. A broadband complex impedance match performance from 5.24 to 6.07 GHz (fractional bandwidth $\approx$ 14.6%) is achieved. Although there is a significant decline in the curve of S11 of Antenna 2 around 9.2 GHz, it also can be seen that the impedance is mismatched within the frequency band of 11 to 12 GHz, which is important for harmonic suppression.

TABLE 2. Comparison With Other CP Filtering Antennas.

Ref No.	Freq(GHz)	Impedance Match	Impedance/AR BW	Gain (dBi)	S11 @ 2-nd harmonic	Front-to-back Ratio
[8]	1.8	50Ω	27.8% (DRA)	6	>-1dB	~15dB
[9]	8	50Ω	6.13% / 3.68%	5.3	Not Given	Not Given
[11]	3.77-4.26	50Ω	12.2%	5.2	Not Given	18dB
[12]	C/X	50Ω	21%@C 21.2%@X / 13.2%@C 12.8@X	14.5@C(2×2array) / 17.5@X(4×4array)	Not Given	~12dB
[13]	10	50Ω	7.6%, 8.3%(2×2array) / 1.3%, 14.7(2×2array)	6.77 / 12.89(2×2array)	Not Given	Not Given
[19]	2.47	50Ω	4.5% / 9.4-10.5%	6.0-6.1	Not Given	19 dB
[20]	4	50Ω	10.3% / 8.8%	5.8	Not Given	Not Given
Antenna 1	5.8	50Ω	18.5% / 8.7%	8.5	>-0.85dB	>18dB
Antenna 2	5.8	Complex Impedance	14.5% / 8.5%	8	>-1dB	>18dB

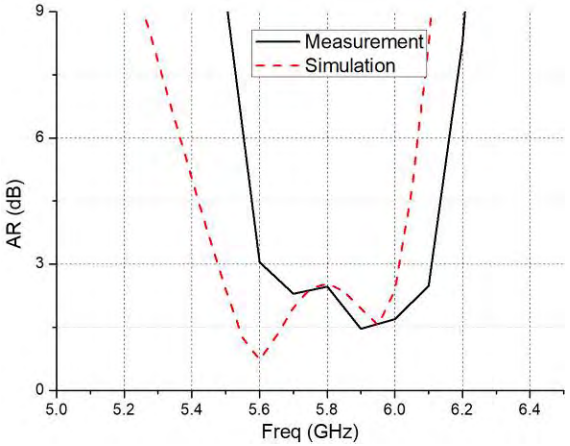

FIGURE 21. Measured and simulated AR of Antenna 2.

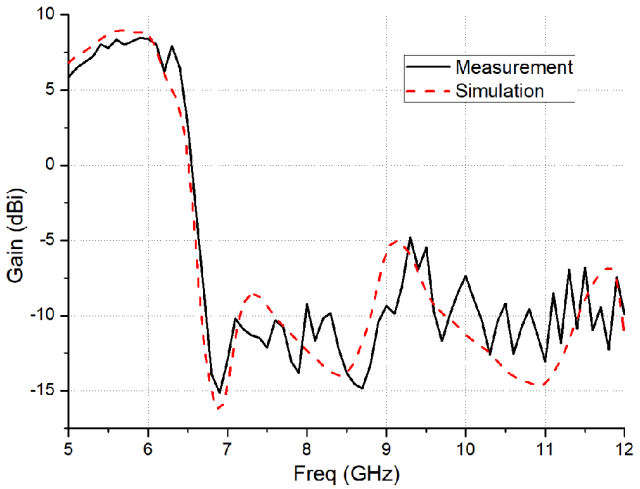

FIGURE 22. Measured and simulated gains of Antenna 2.

The characteristic impedance of the measurement system in the anechoic chamber is 50 Ω. In order to measure the radiation performance of Antenna 2 with the complex impedance, an open-shunt stub is introduced to match the impedance of Antenna 2 to the 50 Ω terminal, as shown in Fig. 20.

The measured AR shown in Fig. 21 is below 3 dB from 5.6 to 6.1 GHz. The difference between measured and simulated results may be attributed to the effect of open-shunt stub and fabrication tolerance. As shown in Fig. 22, this LHCP antenna exhibits a flat gain response of more than 8 dBic from 5.6 to 6.1 GHz. The gain decreases by more than 15 dB from 11 to 12 GHz, showing good harmonic radiation suppression.

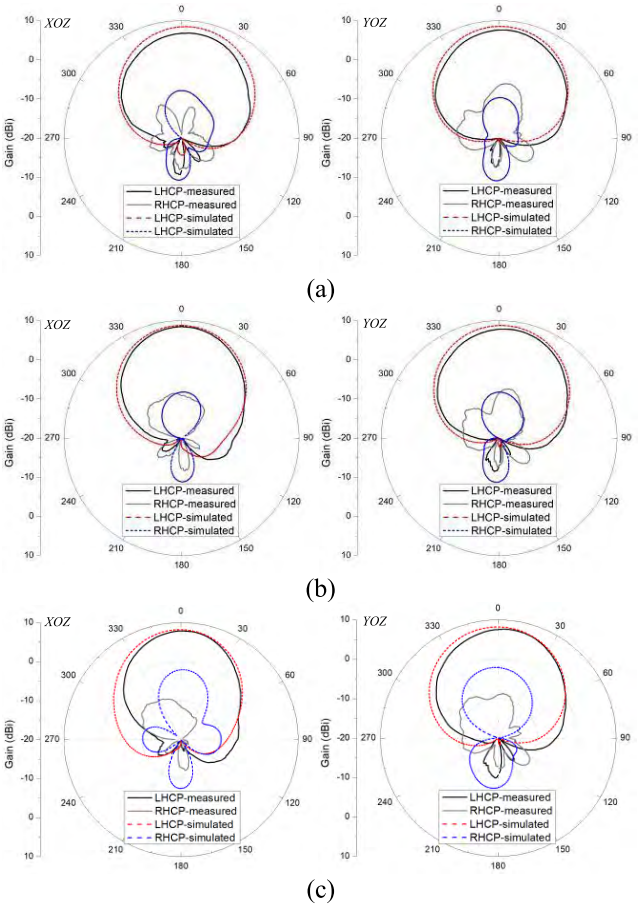

FIGURE 23. Radiation patterns of Antenna 2 in both the XOZ plane and YOZ plane: (a) 5.6 GHz; (b) 5.8 GHz; (c) 6.1 GHz.

The simulated and measured radiation patterns Antenna 2 in both the *XOZ* plane ($\phi = 0°$) and *YOZ* plane ($\phi = 90°$) at 5.6, 5.8, and 6.1 GHz are shown in Fig. 23. The measured XPD in the broadside direction and the front-to-back ratio are similar to Antenna 1 with values of more than 16 and 18 dB, respectively.

The comparison between the proposed antennas and other CP filtering antennas reported in the literature is summarized in Table 2. It can be seen that the proposed antenna can

realize 50 Ω and complex impedance matching to RF circuits with wide impedance and AR bandwidths while maintaining high gain, high front-to-back ratio and good 2nd harmonic suppression.

IV. CONCLUSION

In this paper, the state-of-the-art CP filtering antennas with wideband operation are reviewed first. Then, a novel design of broadband integrated filtering antenna based on EMSIW resonators is proposed for rectenna application. Several important problems of the application of the filtering antenna in rectenna are addressed in this paper: 1) complex impedance match to eliminate the impedance match network with rectifying circuits; 2) using high-Q EMSIW resonators to increase antenna gain; 3) improving front-to-back ratio to enhance efficiency. This concept and design also have good application prospects in active antennas and RFID techniques.

REFERENCES

[1] C.-T. Chuang and S.-J. Chung, "Synthesis and design of a new printed filtering antenna," *IEEE Trans. Antennas Propag.*, vol. 59, no. 3, pp. 1036–1042, Mar. 2011.

[2] Y. Yusuf and X. Gong, "A new class of 3-D filter/antenna integration with high quality factor and high efficiency," in *IEEE MTT-S Int. Microw. Symp. Dig.*, May 2010, pp. 892–895.

[3] H. Chu and Y.-X. Guo, "A filtering dual-polarized antenna subarray targeting for base stations in millimeter-wave 5G wireless communications," *IEEE Trans. Compon., Packag., Manuf. Technol.*, vol. 7, no. 6, pp. 964–973, May 2017.

[4] X. Y. Zhang, Y. Zhang, Y.-M. Pan, and W. Duan, "Low-profile dual-band filtering patch antenna and its application to LTE MIMO system," *IEEE Trans. Antennas Propag.*, vol. 65, no. 1, pp. 103–113, Jan. 2017.

[5] C.-X. Mao *et al.*, "An integrated filtering antenna array with high selectivity and harmonics suppression," *IEEE Trans. Microw. Theory Techn.*, vol. 64, no. 6, pp. 1798–1805, Jun. 2016.

[6] C.-X. Mao *et al.*, "Integrated dual-band filtering/duplexing antennas," *IEEE Access*, vol. 6, pp. 8403–8411, 2018.

[7] S. Gao, Q. Luo, and F. G. Zhu, *Circularly Polarized Antennas*. Hoboken, NJ, USA: Wiley, 2013.

[8] B. J. Xiang, S. Y. Zheng, Y. M. Pan, and Y. X. Li, "Wideband circularly polarized dielectric resonator antenna with bandpass filtering and wide harmonics suppression response," *IEEE Trans. Antennas Propag.*, vol. 65, no. 4, pp. 2096–2101, Apr. 2017.

[9] A. K. Sahoo, R. D. Gupta, and M. S. Parihar, "Circularly polarised filtering dielectric resonator antenna for X-band applications," *IET Microw., Antennas Propag.*, vol. 12, no. 9, pp. 1514–1518, Jul. 2018.

[10] W. Cheng and D. Li, "Circularly polarised filtering monopole antenna based on miniaturised coupled filter," *Electron. Lett.*, vol. 53, no. 11, pp. 700–702, May 2017.

[11] Z. H. Jiang and D. H. Werner, "A compact, wideband circularly polarized co-designed filtering antenna and its application for wearable devices with low SAR," *IEEE Trans. Antennas Propag.*, vol. 63, no. 9, pp. 3808–3818, Sep. 2015.

[12] C.-X. Mao, S. Gao, Y. Wang, Q.-X. Chu, and X.-X. Yang, "Dual-band circularly polarized shared-aperture array for C-/X-band satellite communications," *IEEE Trans. Antennas Propag.*, vol. 65, no. 10, pp. 5171–5178, Oct. 2017.

[13] T. Li and X. Gong, "Vertical integration of high-Q filter with circularly polarized patch antenna with enhanced impedance-axial ratio bandwidth," *IEEE Trans. Microw. Theory Techn.*, vol. 66, no. 6, pp. 3119–3128, Jun. 2018.

[14] P. F. Hu, Y. M. Pan, X. Y. Zhang, and S. Y. Zheng, "A compact filtering dielectric resonator antenna with wide bandwidth and high gain," *IEEE Trans. Antennas Propag.*, vol. 64, no. 8, pp. 3645–3651, Aug. 2016.

[15] P. F. Hu, Y. M. Pan, K. W. Leung, and X. Y. Zhang, "Wide-/dual-band omnidirectional filtering dielectric resonator antennas," *IEEE Trans. Antennas Propag.*, vol. 66, no. 5, pp. 2622–2627, May 2018.

[16] N. Yang, C. Caloz, and K. Wu, "Co-designed CPS UWB filter-antenna system," in *Proc. IEEE AP-S Int. Symp.*, Jun. 2007, pp. 1433–1436.

[17] C.-T. Chuang and S.-J. Chung, "A compact printed filtering antenna using a ground-intruded coupled line resonator," *IEEE Trans. Antennas Propag.*, vol. 59, no. 10, pp. 3630–3637, Oct. 2011.

[18] X. Chen, F. Zhao, L. Yan, and W. Zhang, "A compact filtering antenna with flat gain response within the passband," *IEEE Antennas Wireless Propag. Lett.*, vol. 12, pp. 857–860, 2013.

[19] Y. Lu, Y. Wang, S. Gao, C. Hua, and T. Liu, "Circularly polarised integrated filtering antenna with polarisation reconfigurability," *IET Microw., Antennas Propag.*, vol. 11, no. 15, pp. 2247–2252, Dec. 2017.

[20] Q.-S. Wu, X. Zhang, and L. Zhu, "Co-design of a wideband circularly polarized filtering patch antenna with three minima in axial ratio response," *IEEE Trans. Antennas Propag.*, vol. 66, no. 10, pp. 5022–5030, Oct. 2018.

[21] P. E. Glaser, "Power from the sun: Its future," *Science*, vol. 162, no. 3856, pp. 857–861, Nov. 1968.

[22] W. C. Brown and E. E. Eves, "Beamed microwave power transmission and its application to space," *IEEE Trans. Microw. Theory Techn.*, vol. 40, no. 6, pp. 1239–1250, Jun. 1992.

[23] N. Shinohara, "Power without wires," *IEEE Microw. Mag.*, vol. 12, no. 7, pp. S64–S73, Dec. 2011.

[24] B. Strassner and K. Chang, "Microwave power transmission: Historical milestones and system components," *Proc. IEEE*, vol. 101, no. 6, pp. 1379–1396, Jun. 2013.

[25] S. Sasaki, K. Tanaka, and K.-I. Maki, "Microwave power transmission technologies for solar power satellites," *Proc. IEEE*, vol. 101, no. 6, pp. 1438–1447, Jun. 2013.

[26] R. Wang *et al.*, "Optimal matched rectifying surface for space solar power satellite applications," *IEEE Trans. Microw. Theory Tech.*, vol. 62, no. 4, pp. 1080–1089, APR. 2014.

[27] Y. Dong *et al.*, "Focused microwave power transmission system with high-efficiency rectifying surface," *IET Microw., Antennas Propag.*, vol. 12, no. 5, pp. 808–813, Apr. 2018.

[28] Y.-Y. Gao, X.-X. Yang, C. Jiang, and J.-Y. Zhou, "A circularly polarized rectenna with low profile for wireless power transmission," *Prog. Electromagn. Res. Lett.*, vol. 13, pp. 41–49, Jan. 2010.

[29] Y. Yang *et al.*, "A circularly polarized rectenna array based on substrate integrated waveguide structure with harmonic suppression," *IEEE Antennas Wireless Propag. Lett.*, vol. 17, no. 4, pp. 684–688, Apr. 2018.

[30] P. Li, H. Chu, and R.-S. Chen, "Design of compact bandpass filters using quarter-mode and eighth-mode SIW cavities," *IEEE Trans. Compon., Packag., Manuf. Technol.*, vol. 7, no. 6, pp. 956–963, Jun. 2017.

[31] Q. Lai, C. Fumeaux, W. Hong, and R. Vahldieck, "Characterization of the propagation properties of the half-mode substrate integrated waveguide," *IEEE Trans. Microw. Theory Techn.*, vol. 57, no. 8, pp. 1996–2004, Aug. 2009.

[32] J. Wu, Y. Yin, Z. Wang, and R. Lian, "Broadband circularly polarized patch antenna with parasitic strips," *IEEE Antennas Wireless Propag. Lett.*, vol. 14, pp. 559–562, 2015.

YAZHOU DONG received the B.S. degree from Xi'an Jiaotong University, Xi'an, China, in 2006, and the M.S. degree from Southeast University, Nanjing, China, in 2009. He is currently pursuing the Ph.D. degree with the School of Electronics and Information, Northwestern Polytechnical University, Xi'an, China. He is also a Senior Engineer with the National Key Laboratory of Science and Technology on Space Microwave, China Academy of Space Technology, Xi'an. Since 2017, he has been a Visiting Researcher at the University of Kent, U.K., supported by the China Scholarship Council. His current research interests include space microwave technologies powered by microwave power transmission, microwave power combining, and antenna array technology.

STEVEN GAO (M'01–SM'16) is currently a Professor and the Chair of RF and Microwave Engineering, University of Kent, U.K. He has authored two books including *Space Antenna Handbook* (Wiley, 2012) and *Circularly Polarized Antennas*(IEEE & Wiley, 2014), over 200 papers, and several patents. His research covers smart antennas, phased arrays, MIMO, satellite antennas, RF/microwave/mm-wave circuits, satellite communications, UWB radars, synthetic-aperture radars, and mobile communications. He was the General Chair of LAPC 2013, and a Keynote Speaker or Invited Speaker at some international conferences, such as AES'2014 (China), IWAT'2014 (Sydney), SOMIRES'2013 (Japan), and APCAP'2014 (China). He is an IEEE AP-S Distinguished Lecturer, an Associate Editor of the IEEE Transactions on Antennas and Propagation, an Associate Editor of *Radio Science*, and the Editor-in-Chief for Wiley Book Series on Microwave and Wireless Technologies.

QI LUO (S'08–M'12) received the M.Sc. degree in data communications from the University of Sheffield, Sheffield, U.K., in 2006, and the Ph.D. degree in electrical engineering from the University of Porto, Porto, Portugal, in 2012. From 2012 to 2013, he was a Research Fellow with the Surrey Space Center, Guildford, U.K. He is currently a Research Associate with the School of Engineering and Digital Arts, University of Kent, Canterbury, U.K. His current research interests include smart antennas, circularly polarized antennas, reflectarray, multiband microstrip antennas, and electrically small antenna design.

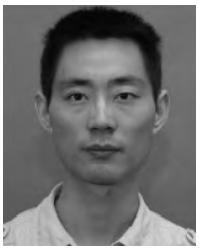

LEHU WEN received the M.S. degree from Xidian University, Xi'an, China, in 2011. He is currently pursuing the Ph.D. degree with the University of Kent, Canterbury. His current research interests include multi-band base station antenna, mobile terminal antenna, and tightly coupled array.

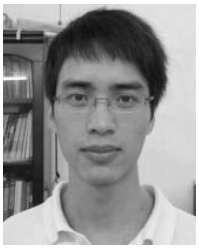

CHUN-XU MAO was born in Hezhou, China. He received the M.S. degree in RF and microwave engineering from the South China University of Technology in 2013 and the Ph.D. degree from the University of Kent, U.K., in 2017. He is currently with the Computational Electromagnetics and Antennas Research Laboratory, Department of Electrical Engineering, Pennsylvania State University, USA, as a Post-Doctoral Research Associate. His research interests include filtering antenna integration, UWB antenna, circularly polarized satellite antenna array, multiband synthetic aperture radar antenna array, multifunctional RF frontend, and wearable antenna.

SHI-WEI DONG (M'10–SM'15) received the B.S. and M.S. degrees in mechanical and electronic engineering and Ph.D. degree in circuitry and system from Northwestern Polytechnical University, Xi'an, China, in 1997, 1999, and 2003, respectively.

He conducted research with the Microwave Technology Department, Xi'an Institute of Space Radio Technology, Xi'an. In 2005, he joined the National Key Laboratory of Science and Technology on Space Microwave, China Academy of Space Technology, Xi'an. He is currently a Senior Engineer involved with space microwave technology. He has authored or co-authored one book and over 30 publications in refereed journals and conference proceedings. His current research interests include high-efficiency PAs, microwave and millimeter-wave power combining, microwave power transmission, and electromagnetic wave propagation.

XIAOJUN LI is currently the Director of the National Key Laboratory of Science and Technology on Space Microwave, China Academy of Space Technology, Xi'an, China.

GAO WEI is currently a Professor with Northwestern Polytechnical University, Xi'an, China.

GEYI WEN (M'88) was born in Hunan, China, in 1963. He received the B.Eng., M.Eng., and Ph.D. degrees in electrical engineering from Xidian University (formerly Northwest Telecommunications Institute), China, in 1982, 1984, and 1987 respectively. From 1998 to 2007, he was with the Radio Frequency Department, Research in Motion Ltd. (now Blackberry Ltd.), Canada, as a Senior Scientist, and then the Director of the Advanced Technology Department. Since 2010, he has been the National Distinguished Professor of China with Fudan University, Shanghai, and then with the Nanjing University of Information Science and Technology (NUIST), Nanjing, China. He is currently the Director of the Research Center of Applied Electromagnetics, NUIST. His current research interests include microwave theory and techniques, and antennas and wave propagation.

YOULIN GENG is currently with Hangzhou Dianzi University, Hangzhou, China.

ZHIQUN CHENG is currently with Hangzhou Dianzi University, Hangzhou, China.